

Medium induced QCD cascades: broadening, entropy and rescattering during branching

E. Blanco^a, K. Kutak^a, W. Płaczek^b, M. Rohrmoser^a and R. Straka^c

^a*Institute of Nuclear Physics, Polish Academy of Sciences,
ul. Radzikowskiego 152, 31-342 Kraków, Poland*

^b*Institute of Applied Computer Science, Jagiellonian University,
ul. Łojasiewicza 11, 30-348 Kraków, Poland*

^c*AGH University of Science and Technology, Kraków, Poland*

Abstract

We study evolution equations describing jet propagation through quark–gluon plasma (QGP). In particular we investigate the contribution of momentum transfer during branching and find that such a contribution is sizeable. Furthermore, we study various approximations, such as the Gaussian approximation and the diffusive approximation to the jet-broadening term. We notice that in order to reproduce the BDIM equation (without the momentum transfer in the branching) the diffusive approximation requires a very large value of the jet-quenching parameter \hat{q} . We also quantify the solutions by calculating time dependence of entropy associated with each of the distributions.

1 Introduction

Quantum Chromodynamics (QCD) is the very well established theory of strong interactions with rich structure and many phases [1]. Here we want to focus on a jet-quenching phenomenon predicted in [2, 3], and observed experimentally at RHIC [4] and LHC [5]. The jet quenching is a suppression of propagation of jets in quark–gluon plasma (QGP) due to jet–plasma interactions. This process has many phases, recently discussed in Refs. [6, 7], see also [8]. The jet-quenching phenomenon is approached from many directions: the kinetic theory [9–18], Monte Carlo methods [19–24], the AdS/CFT [25]. Furthermore, it is a multi-scale problem which, however, allows for factorisation in time. In particular, according to Refs. [6, 7], in the first phase the jet propagates according to the vacuum-like parton shower with ordering in an angle, while in the next stage the coherence is broken and jet propagates through plasma experiencing elastic scatterings and branching – in this stage there are many soft radiations and wide-angle emissions. In the last stage, when jet leaves medium, again the vacuum-like emissions dictate its time evolution. In this paper, we focus on the second phase of the jet propagation through QGP. In particular, we investigate what is the contribution of momentum transfer during branching to the broadening pattern of the jet. To address this problem, we solve the equation proposed in [26, 27] which is a generalised version of the equation solved by three of us in Ref. [28]¹. In this approach, QGP is modelled by static centres and the jet interacts with it weakly, jet propagating through plasma branches according to BDMPS-Z mechanism [9–18] and gets broader due to elastic scattering with plasma.

In Ref. [28] we observed that accounting for the broadening term beyond the diffusive approximation leads to the non-Gaussian broadening for jet observables. In particular, we studied the azimuthal angle decorrelation of di-jet produced in central–forward rapidity region. It turns out that the non-Gaussianity leads to much stronger broadening of the cross section for decorrelations than the Gaussian approximation.

In the current study, we see that the momentum exchange during branching has non-negligible contribution to the broadening, therefore such a contribution should not be neglected. Experimentally, the broadening is rather small and its observation at the LHC energies is hindered by the vacuum effects [30, 31]. There are also possible effects which could give negative contribution to the broadening [32–34]. Furthermore, a more realistic model of the medium accounting for its expansion [33, 35, 36] will probably reduce the amount of the broadening. While at present we do not account for a more realistic scenario, i.e. the expansion of the medium we mimic it by scaling the \hat{q} parameter. We observe that reducing its value leads to the smaller broadening. To quantify the difference between distributions, we calculate the so-called Δ -entropy. It shows that increased broadening leads to generation of the larger entropy.

The paper is organised as follows: In Section 2 we discuss the version of the transverse-momentum-dependent BDIM (Blaziot, Dominguez, Iancu, Mehtar-Tani) equation [27] where the momentum transfer in the kernel is taken into account and we present its solution with the use of Monte Carlo methods. In Section 3 we compare the BDIM equation to some of its approximations, i.e. the case where transverse momentum in the branching kernel is neglected, the

¹For other approach which addresses the transverse-momentum dependence but neglects the large- x parton’s spectrum see the relaxing harmonic approximation of Ref. [29].

case when the broadening term is represented by the diffusive approximation, and the Gaussian approximation where the transverse momentum and the longitudinal momentum are factorised. In Section 4 we calculate entropy associated with the obtained distributions. We use the so-called Δ -entropy S_Δ which is a discrete approximation of the differential entropy. While we are aware that this cannot be directly linked to the observed multiplicity of the final state, we see some interesting features, like: rapid growth at initial times, saturation at longer times and direct proportionality between the broadening and the amount of the entropy. We conclude our work in Section 5. In Appendix A we present one of the Monte Carlo algorithms for solving the full BDIM equation², while in Appendix B we describe a numerical method used to solve the diffusive approximation of the BDIM equation.

2 Momentum-transfer-dependent BDIM equation and its solution

The evolution equation for the gluon transverse-momentum-dependent distribution $D(x, \mathbf{k}, t)$ in the dense medium reads [27]

$$\begin{aligned} \frac{\partial}{\partial t} D(x, \mathbf{k}, t) = & \alpha_s \int_0^1 dz \int \frac{d^2 q}{(2\pi)^2} \left[2\mathcal{K}(\mathbf{Q}, z, \frac{x}{z} p_0^+) D\left(\frac{x}{z}, \mathbf{q}, t\right) - \mathcal{K}(\mathbf{q}, z, x p_0^+) D(x, \mathbf{k}, t) \right] \\ & + \int \frac{d^2 \mathbf{l}}{(2\pi)^2} C(\mathbf{l}) D(x, \mathbf{k} - \mathbf{l}, t). \end{aligned} \quad (1)$$

The kernel $\mathcal{K}(\mathbf{Q}, z, x p_0^+)$ which accounts for the momentum-dependent medium induced branching is given by

$$\mathcal{K}(\mathbf{Q}, z, p_0^+) = \frac{2}{p_0^+} \frac{P_{gg}(z)}{z(1-z)} \sin \left[\frac{\mathbf{Q}^2}{2k_{br}^2} \right] \exp \left[-\frac{\mathbf{Q}^2}{2k_{br}^2} \right] \quad (2)$$

with

$$\omega = x p_0^+, \quad k_{br}^2 = \sqrt{\omega_0 \hat{q}_0}, \quad \mathbf{Q} = \mathbf{k} - z \mathbf{q}, \quad \omega_0 = z(1-z) p_0^+ \quad (3)$$

and

$$\hat{q}_0 = \hat{q} f(z), \quad f(z) = 1 - z(1-z), \quad P_{gg}(z) = N_c \frac{[1 - z(1-z)]^2}{z(1-z)}. \quad (4)$$

where $p_0^+ \equiv E$ is energy of jet entering the medium, x – is longitudinal momentum fraction of mini jet, $\mathbf{k} = (k_x, k_y)$ – is transverse-momentum vector of mini jet, \hat{q} – the quenching parameter, α_s – the QCD coupling constant and N_c – the number of colours.

The elastic collision kernel $C(\mathbf{l})$ is given by

$$C(\mathbf{l}) = w(\mathbf{l}) - \delta(\mathbf{l}) \int d^2 \mathbf{l}' w(\mathbf{l}'), \quad (5)$$

where the function $w(\mathbf{l})$ models the momentum distribution of medium quasi-particles. We consider two scenarios:

²The other one is an extension of the algorithm employed in the Monte Carlo program MINCAS, described in Ref. [28], and will be presented elsewhere.

1. The out-of-equilibrium distribution [27]:

$$w(\mathbf{l}) = \frac{16\pi^2\alpha_s^2 N_c n}{\mathbf{l}^4}, \quad (6)$$

with $\mathbf{l} = (l_x, l_y)$ being transverse-momentum vector and n – the density of scatterers.

2. The situation where the medium equilibrates and the transverse-momentum distribution assumes the form obtained from the Hard Thermal Loops (HTL) calculation [37]. In this case the medium is characterised by a mass scale given by the Debye mass m_D :

$$w(\mathbf{l}) = \frac{g^2 m_D^2 T}{\mathbf{l}^2 (\mathbf{l}^2 + m_D^2)}, \quad (7)$$

$$m_D^2 = g^2 T^2 \left(\frac{N_c}{3} + \frac{N_f}{6} \right), \quad g^2 = 4\pi\alpha_s.$$

The equation (1) has been solved using the Monte Carlo program MINCAS by extending the algorithm presented in [28] (to be described elsewhere) and, independently, using another Monte Carlo algorithm described in the Appendix A. The two solutions have been checked to be in a good numerical agreement. Here we present the results from MINCAS obtained using the following input parameters:

$$\begin{aligned} x_{\min} &= 10^{-4}, & \varepsilon &= 10^{-6} \\ q_{\min} &= 0.1 \text{ GeV}, & m_D &= 0.993 \text{ GeV}, & \sigma_{k_0} &= 0 \text{ GeV}, \\ N_c &= 3, & \bar{\alpha}_s &= 0.3, \\ E &= 100 \text{ GeV}, & n &= 0.243 \text{ GeV}^3, & \hat{q} &= 1 \text{ GeV}^2/\text{fm}. \end{aligned}$$

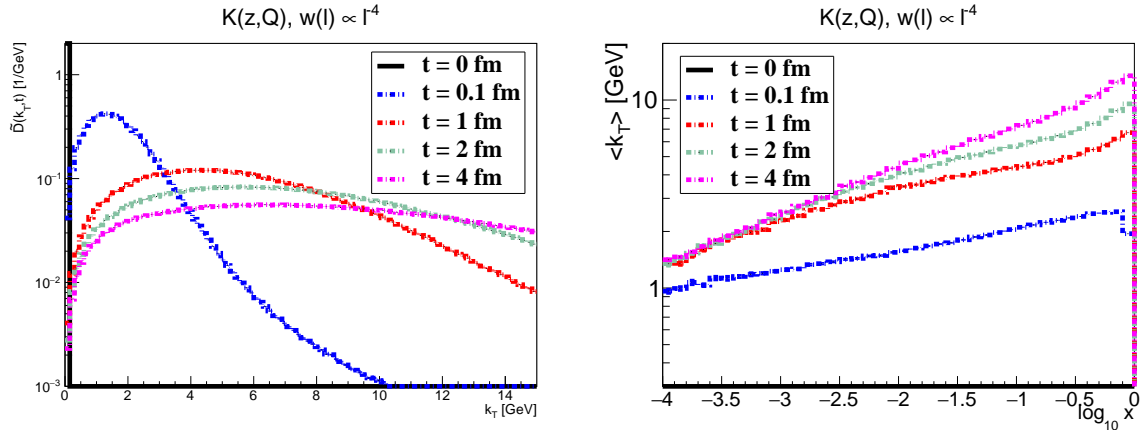


Figure 1: The k_T and $\langle k_T \rangle$ vs. $\log_{10} x$ distributions for the evolution time values $t = 0, 0.1, 1, 2, 4$ fm, for the full kernel $\mathcal{K}(z, \mathbf{Q})$ and the collision terms of Eq. (6).

In Fig. 1 we show the k_T distributions as well as $\langle k_T \rangle$ as a function of x for the evolution time values $t = 0, 0.1, 1, 2, 4$ fm. The detailed discussion of the solution is presented in the next section where we also discuss comparisons to the approximations of the BDIM equation.

3 Comparison of BDIM equation to its approximations

In this section we will discuss various approximations of the BDIM equation.

- The first approximation that we consider is the case when the momentum transfer during branching is neglected. In this case, as demonstrated in Ref. [26], the branching kernel simplifies to a purely collinear one and the transverse momentum dependence comes basically from the elastic scattering. The equation reads

$$\begin{aligned} \frac{\partial}{\partial t} D(x, \mathbf{k}, t) = & \frac{1}{t^*} \int_0^1 dz \mathcal{K}(z) \left[\frac{1}{z^2} \sqrt{\frac{z}{x}} D\left(\frac{x}{z}, \frac{\mathbf{k}}{z}, t\right) \theta(z-x) - \frac{z}{\sqrt{x}} D(x, \mathbf{k}, t) \right] \\ & + \int \frac{d^2 \mathbf{q}}{(2\pi)^2} C(\mathbf{q}) D(x, \mathbf{k} - \mathbf{q}, t), \end{aligned} \quad (8)$$

where

$$\mathcal{K}(z) = \frac{(1-z+z^2)^{5/2}}{[z(1-z)]^{3/2}}, \quad \frac{1}{t^*} = \frac{\alpha_s N_c}{\pi} \sqrt{\frac{\hat{q}}{p_0^+}}. \quad (9)$$

- One can further simplify the BDIM equation by expanding the elastic collision term and using the diffusive approximation [26] to obtain

$$\begin{aligned} \frac{\partial}{\partial t} D(x, \mathbf{k}, t) = & \frac{1}{t^*} \int_0^1 dz \mathcal{K}(z) \left[\frac{1}{z^2} \sqrt{\frac{z}{x}} D\left(\frac{x}{z}, \frac{\mathbf{k}}{z}, t\right) \theta(z-x) - \frac{z}{\sqrt{x}} D(x, \mathbf{k}, t) \right] \\ & + \frac{1}{4} \hat{q} \nabla_k^2 \left[D(x, \mathbf{k}, t) \right]. \end{aligned} \quad (10)$$

In the above equation, as compared to Ref. [26], we have neglected the mild logarithmic dependence of \hat{q} in the diffusion term on k_T .

- Eq. (10) was also solved approximately in Ref. [38]. To arrive at the solution, the branching term was neglected and the Gaussian ansatz was used. The solution reads

$$D(x, \mathbf{k}, t) = D(x, t) \frac{4\pi}{\langle k_\perp^2 \rangle} \exp \left[-\frac{\mathbf{k}^2}{\langle k_\perp^2 \rangle} \right], \quad (11)$$

where

$$\langle k_\perp^2 \rangle = \min \left\{ \frac{1}{2} \hat{q} t (1+x^2), \frac{k_{br}^2(x)}{4\bar{\alpha}}, (xE)^2 \right\}, \quad k_{br}^2(x) = \sqrt{x E \hat{q}}. \quad (12)$$

In the above, it is assumed that $k_\perp^2 < \omega^2 = (xE)^2$, and the parameters are: $\bar{\alpha}_s = 0.3$, $\hat{q} = 1 \text{ GeV}^2/\text{fm}$, $E = 100 \text{ GeV}$.

Similarly to Eq. (1), Eq. (8) has been solved using the Monte Carlo programs, basically re-obtaining the result from Ref. [28], while Eq. (10) has been solved with the help of the numerical method described in Appendix B. For Eq. (1) and Eq. (8) we have used both the functions $w(\mathbf{l})$ from Eqs. (6) and (7) to describe the collision term when using both the full kernel and the

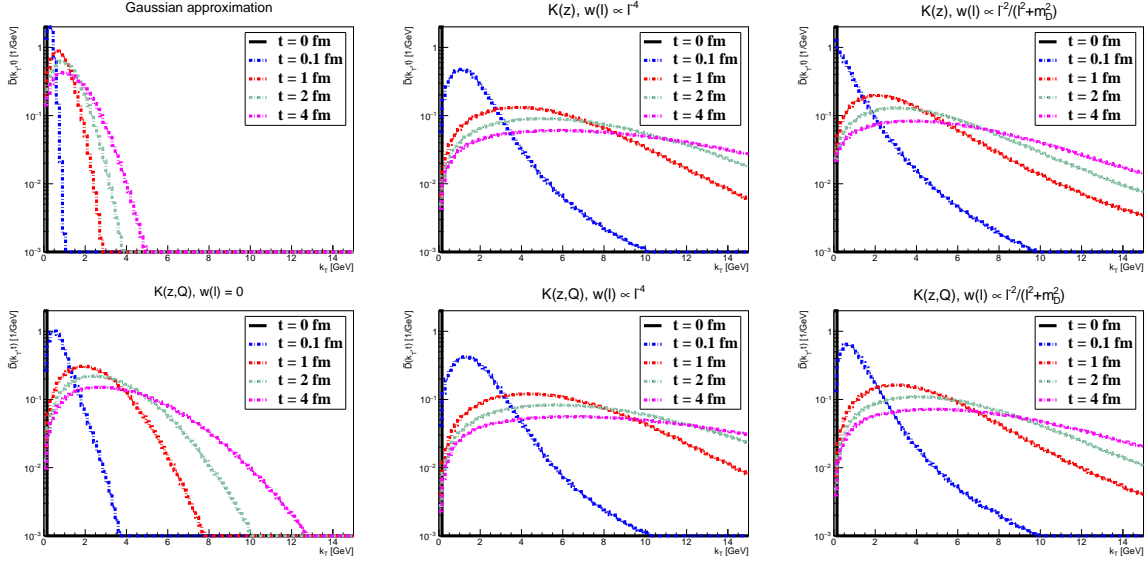


Figure 2: The k_T distributions for the evolution time values $t = 0, 0.1, 1, 2, 4$ fm, for different kernels: the Gaussian approximation, $\mathcal{K}(z)$ and $\mathcal{K}(z, \mathbf{Q})$, and different collision terms: no collision term, the collision term as in Eq. (6) and as in Eq. (7).

simplified one. In the case of the full kernel, we have also performed calculations without the collision term. For all the the presented results, we have used the parameters given in the previous section.

In Fig. 2 we show the k_T distributions of the six cases studied for evolution time values $t = 0, 0.1, 1, 2, 4$ fm. We directly notice that the Gaussian approximation fails to describe any of the other results. The nearest distribution is the one with the full kernel and no collision term, which approaches a Gaussian shape, but with a much wider width. The other distributions (with the collision term) show fast broadening of the initial Dirac- δ -like distribution, exhibiting the non-Gaussian shape. The broadening is faster with $w(\mathbf{l})$ given by Eq. (6) than with the one given by Eq. (7), i.e the broadening is faster with out-of-equilibrium momentum distributions of the medium quasi-particles.

In Fig. 3 we present the dependence of $\langle k_T \rangle$ (the mean value of k_T) on $\log_{10} x$. For all cases, $\langle k_T \rangle$ grows with time and with x . It is still true for the Gaussian approximation, even if the distribution for the different evolution time join each other under certain values of x . We can clearly see in these figures a different behaviour around $x = 1$ between the distributions corresponding to the z -only dependent kernel and the ones corresponding to the full kernel which show a drop. Before this drop, these distribution increase with x , while this is true only for long evolution time with the z dependent kernel only. More generally, $\langle k_T \rangle$ is higher with the full kernel than with the z -only dependent one.

An interesting question is what is the domain of applicability of the diffusive approximation that was used in order to reduce Eq. (8) to Eq. (10). The approximation is advocated as a systematic expansion around k_T and should be valid for rather low values of k_T . From Fig. 4 we see that the solution of the Eq. (10) is reasonably reproduced in the diffusive approximation,

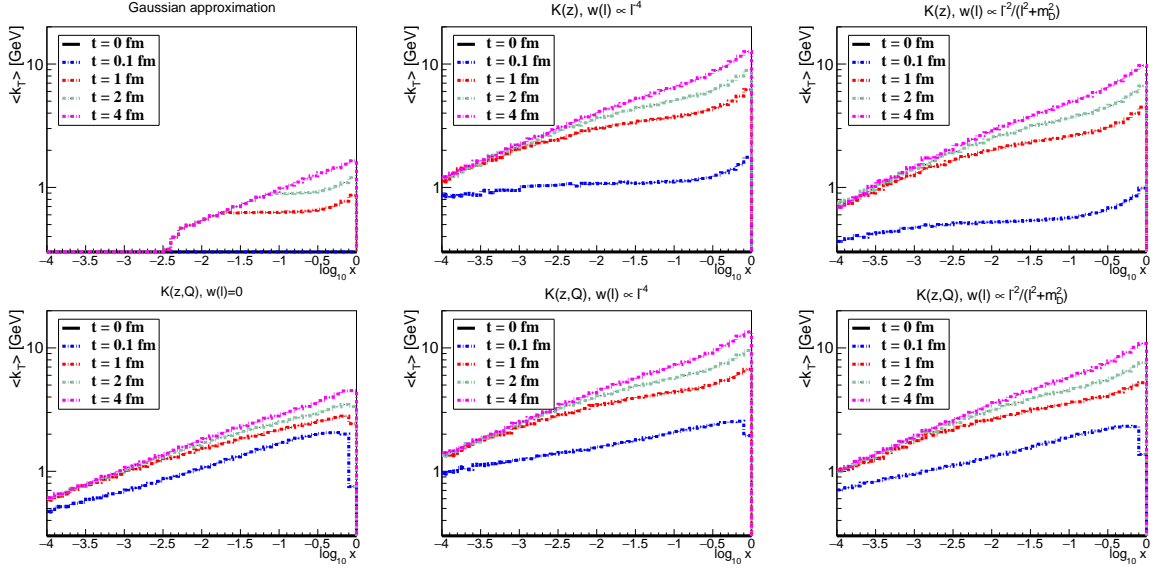


Figure 3: The $\langle k_T \rangle$ vs. $\log_{10} x$ distributions for the evolution time values $t = 0, 0.1, 1, 2, 4$ fm, for different kernels: the Gaussian approximation, $\mathcal{K}(z)$ and $\mathcal{K}(z, \mathbf{Q})$, and different collision terms: no collision term, the collision term as in Eq. (6) and in Eq. (7), respectively.

only if the \hat{q} is very large. We see, however, that the diffusive approximation preserves the general pattern of Eq. (8), but is much narrower than the solution of the equation before the expansion. This feature is better visible in the plot of the $\langle k_T \rangle$ as a function of x which we show for different values of \hat{q} as well as for different values of t . From these results we conclude that, while the diffusive approximation is qualitatively fine, it is rather crude quantitatively.

To complete the analysis of the k_T spectrum we study its dependence on \hat{q} for the three cases of $\hat{q} = 0.5, 1, 2$ GeV²/fm. We see that, in general, it is not a trivial dependence, in a sense that increasing \hat{q} will just broaden the distribution. This is the case only for the Gaussian approximation and $w(\mathbf{l}) = 0$. The interpretation of this is the following. In these two cases \hat{q} enters to some extent trivially: in the former case as a factor modifying $\langle k_{br}^2 \rangle$, while in the latter in the branching term only. In the remaining cases \hat{q} which controls the broadening enters the branching kernel and is hidden in both the branching term and the elastic scattering term. Interplay of these two effects results in the structure visible in the remaining cases.

4 Entropy

Production of entropy in hadronic collisions is a subject of intense research [39–50]. In particular, some properties of entropy, like its saturation, can signal thermalisation of QGP [39]. This can be also related to properties of the Boltzmann transport equation for which one can define the H function, which measures how fast the equilibrium is approached. Since the equations that we are solving are not complete in a sense of describing simultaneous evolution of medium and jet, like for instance in Ref. [10] (for an overview see Ref. [8] and references therein), we

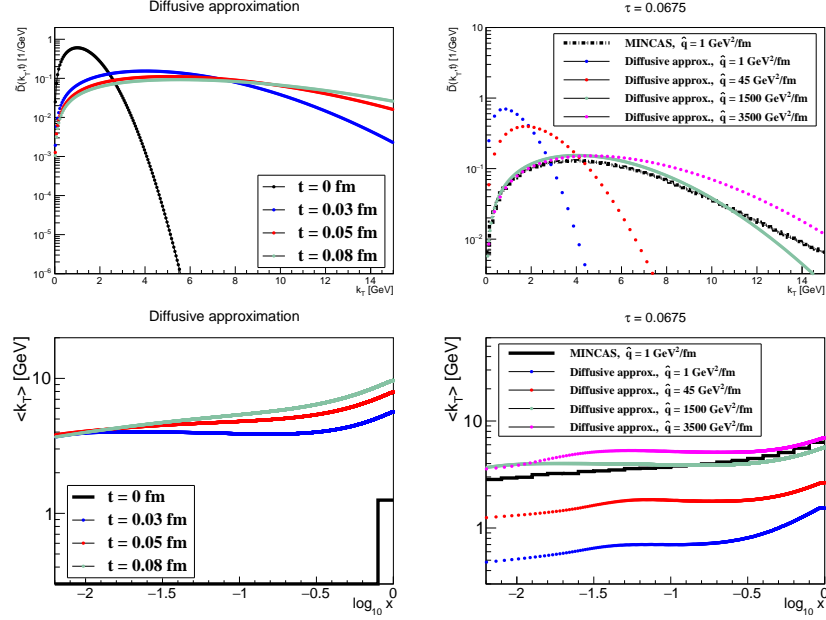


Figure 4: The k_T and $\langle k_T \rangle$ vs. $\log_{10} x$ distributions for the diffusive approximation: for four values of the evolution time $t = 0, 0.03, 0.05, 0.08$ fm and $\hat{q} = 1500 \text{ GeV}^2/\text{fm}$ (left), and for different values of \hat{q} compared with the MINCAS results for $\hat{q} = 1 \text{ GeV}^2/\text{fm}$ and $t = 1$ fm with the z -only dependent kernel $\mathcal{K}(z)$ and the collision term of Eq. (6) (right). In the diffusive approximation $\sigma_{k_0} = 1 \text{ GeV}$ was used; note also that the evolution times for $\hat{q} = 1500 \text{ GeV}^2/\text{fm}$ are equal to $t = 0, 1, 2, 3$ fm ($\tau \equiv t/t^* = 0.0675$ when $t = 1$ fm) in the case of $\hat{q} = 1 \text{ GeV}^2/\text{fm}$.

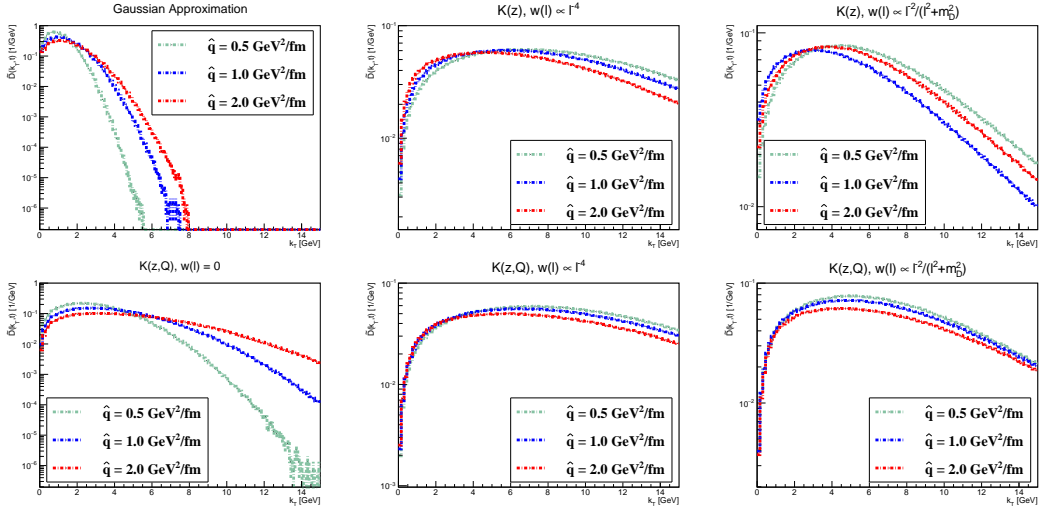


Figure 5: The k_T distributions for $\hat{q} = 0.5, 1, 2 \text{ GeV}^2/\text{fm}$ and $t = 4$ fm.

shall not be able to answer the question about the complete thermalisation of QGP and jets. However, the distribution which is a solution of the BDIM equation defines a probability distribution function and we can quantify what is the entropy associated with it, and whether it

saturates. In this sense we will be able to calculate the entropy associated with gluonic minijets produced by the branching of the leading jet traversing QGP. Furthermore, the interesting point is that having this distribution, one can study the time evolution of the entropy and its dependence on various parameters characterising the system (see Refs. [39, 46] for other approaches to the entropy production problem).

Since our distributions are provided in terms of histograms produced in Monte Carlo simulations, we employ the concept of the so-called Δ -entropy S_Δ which is a discrete approximation of the differential entropy for continuous probability distributions, see e.g. [51]:

$$S_\Delta(t) = - \sum_{i=1}^N p_i(x, k_T, t) \ln p_i(x, k_T, t) + P(t) \ln [\Delta x \Delta k_T], \quad (13)$$

where i is the bin number and N is the total number of bins of the 2D histogram (x, k_T) , while

$$p_i(x, k_T, t) = [\tilde{D}(x, k_T, t) \Delta x \Delta k_T]_i = [2\pi k_T D(x, k_T, t) \Delta x \Delta k_T]_i \quad (14)$$

is the probability of finding a gluon in the i -th bin of the size $\Delta x \Delta k_T$, and

$$P(t) = \sum_{i=1}^N p_i(x, k_T, t). \quad (15)$$

Since in our MC simulations we impose the condition $x \geq x_{\min}$, $P(t)$ is a non-increasing function of t satisfying: $P(t = 0) = 1$ and $P(t > 0) \leq 1$. In fact, it decreases with the evolution time as more and more gluons get stuck in the medium, i.e. their $x < x_{\min}$.

The corresponding differential entropy reads

$$S(t) = - \int dx dk_T \tilde{D}(x, k_T, t) \ln \tilde{D}(x, k_T, t). \quad (16)$$

The results of the Δ -entropy S_Δ as a function of the evolution time are shown in Fig. 6 for the various models of k_T -broadening and three different values of the quenching parameter \hat{q} : $0.5 \text{ GeV}^2/\text{fm}$ (upper panels), $1 \text{ GeV}^2/\text{fm}$ (middle panels) and $2 \text{ GeV}^2/\text{fm}$ (lower panels). Actually, we present the subtracted Δ -entropy $S_\Delta(t) - S_\Delta(0)$, as here we are interested in change of the entropy with time and not in its absolute scale. In general, the Δ -entropy follows an increase for time-scales up to 2 fm to 3 fm, where it starts to saturate. In the cases for $\hat{q} = 2 \text{ GeV}^2/\text{fm}$ the Δ -entropy even starts to decrease at larger time-scales. For the various models of the k_T -broadening it appears that the larger the overall broadening in the k_T distribution is, the larger the increase in entropy is. This behaviour can be verified by comparing different curves in Fig. 6, where the different models observe the same order in k_T -broadening as in entropy increase. From the smallest k_T -broadening/entropy increase to largest, this order is:

1. the Gaussian approximation,
2. the model with the transverse-momentum-dependent splitting $K(z, Q)$ and no scattering kernel,

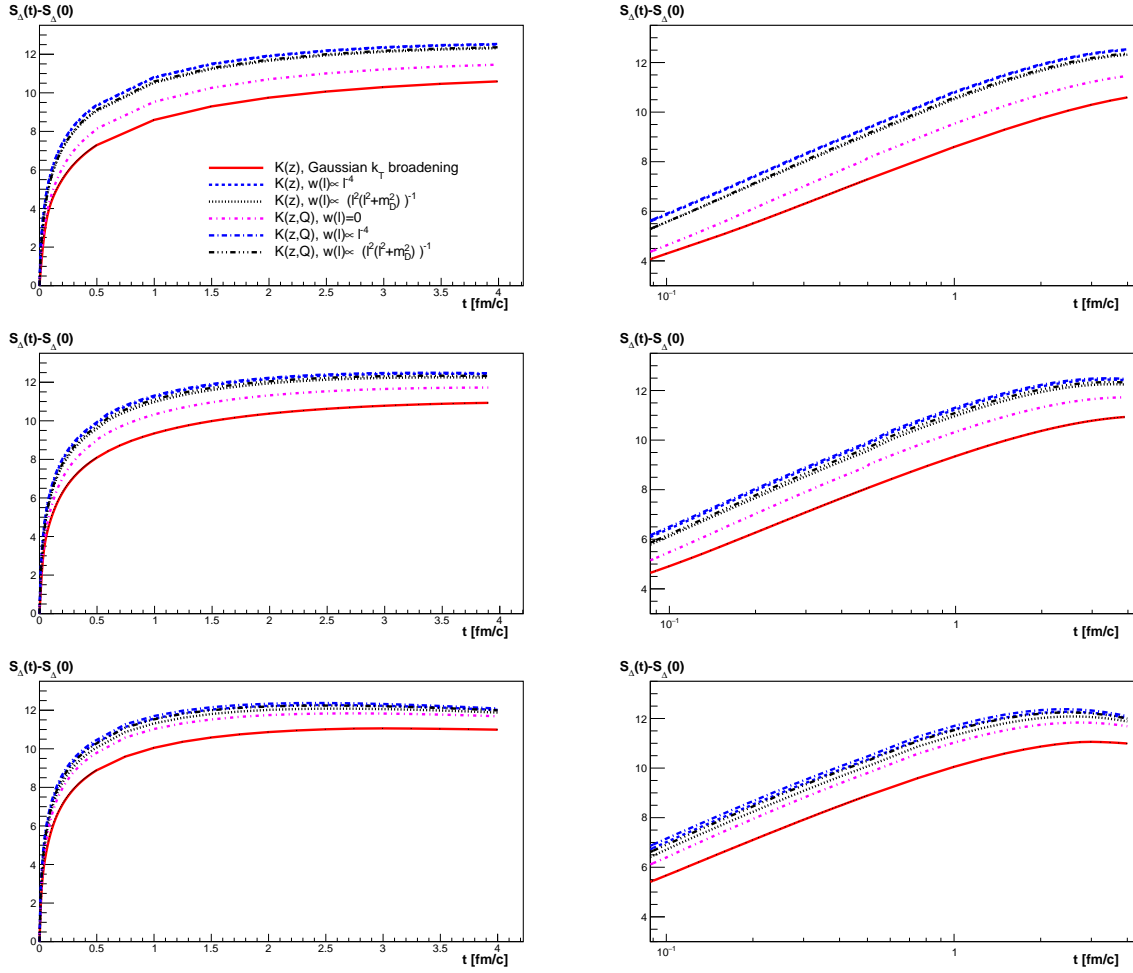


Figure 6: The subtracted Δ -entropy $S_\Delta(t) - S_\Delta(0)$ for different cases of the k_T -broadening as indicated, inside the medium with the quenching parameter $\hat{q} = 0.5 \text{ GeV}^2/\text{fm}$ (upper panels), $\hat{q} = 1 \text{ GeV}^2/\text{fm}$ (middle panels) and $\hat{q} = 2 \text{ GeV}^2/\text{fm}$ (lower panels) shown against the linear (left panels) and logarithmic (right panels) time-scale.

3. the model with the scattering kernel given by $w(\mathbf{l}) \propto 1/[l^2(l^2 + m_D^2)]$ and with the collinear splitting kernel $K(z)$,
4. the model with the scattering kernel as above, but the k_T -dependent splitting kernel $K(z, Q)$,
5. the model with the scattering kernel given by $w(\mathbf{l}) \propto 1/l^4$ and with the collinear splitting kernel $K(z)$,
6. the model with the scattering kernel as above, but with the transverse-momentum-dependent splitting kernel $K(z, Q)$.

It can be argued that this dependence of the entropy on the k_T -broadening is to be expected.

Since the distributions of the longitudinal momentum fraction x , integrated over k_T , are the same in all the cases (as shown in Fig. 7), the differences in the entropy are driven by the changes in the k_T -broadening: the broader the k_T -distribution is, the more different gluon configurations are possible, and thus the entropy is larger.

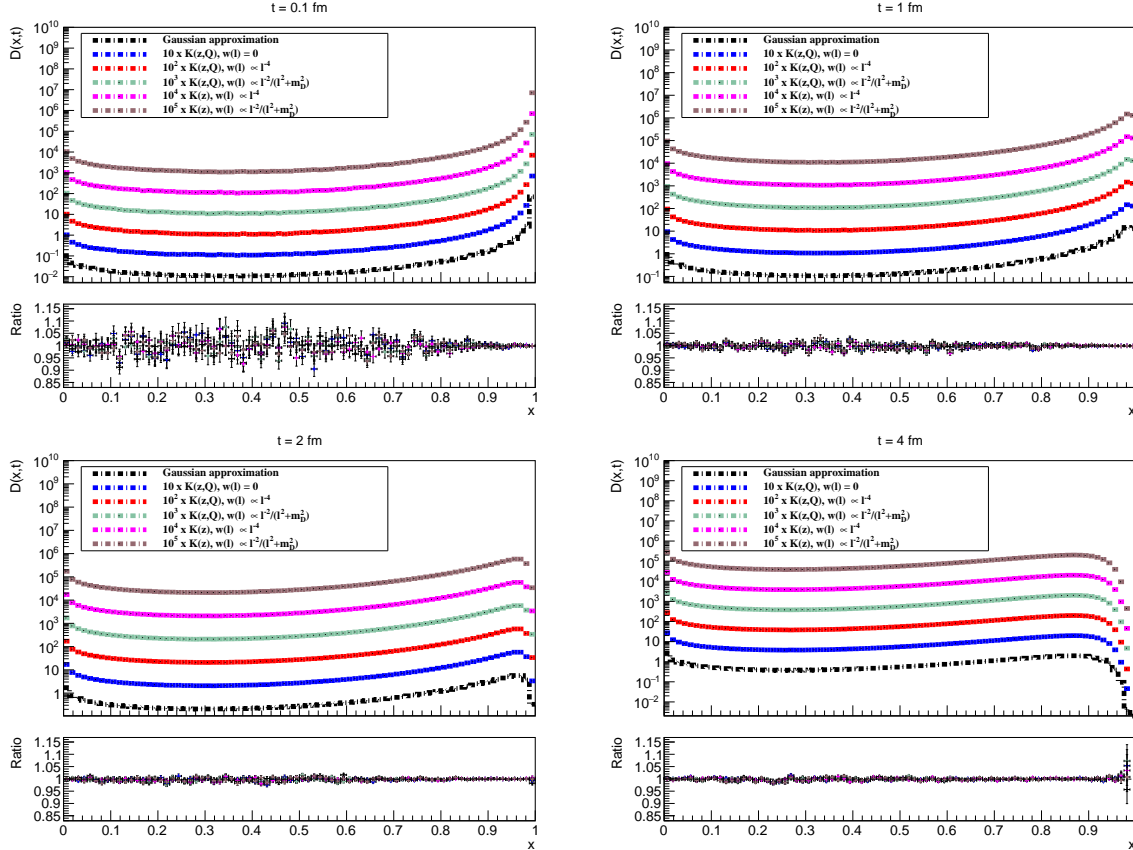


Figure 7: The integrated x distributions (multiplied by the factors 10^n , $n = 0, \dots, 5$) for the evolution time values $t = 0.1, 1, 2, 4$ fm, for different kernels: the Gaussian approximation, $\mathcal{K}(z)$ and $\mathcal{K}(z, \mathbf{Q})$, and different collision terms: no collision term, the collision term as in Eq. (6) and as in Eq. (7). The reference distribution used for the ratio plots is the one for the full kernel $\mathcal{K}(z, \mathbf{Q})$ and the collision term of Eq. (6).

The RHS panels of Fig. 6 show the behaviour of the Δ -entropy S_Δ over logarithmic timescales. It can be seen that before the curves start to saturate, the increase of S_Δ with time is approximately logarithmic.

Comparing the Δ -entropy results for different values of \hat{q} , one can notice that the increase of S_Δ at early timescales is larger for larger values of \hat{q} .

Furthermore, the onset of saturation occurs earlier for higher values of \hat{q} .

5 Conclusions and outlook

We have solved and studied the BDIM equation as well as its various approximations, i.e. the no-momentum-transfer approximation, the diffusive approximation and the Gaussian approximation. We conclude that the momentum transfer during branching gives additional broadening that is non-negligible. Furthermore, the diffusive approximation of the elastic scattering kernel is a rather crude approximation to the BDIM equation.

We have also calculated the entropy corresponding to the (x, k_T) -distributions and we have observed that the largest entropy is the signal of the largest broadening. We have also noticed that for the phenomenologically relevant value of the quenching parameter $\hat{q} = 1 \text{ GeV}^2/\text{fm}$, the entropy calculated for the BDIM equation, both with and without the momentum transfer during the branching, saturates already at the time around 2.5 fm and then slowly decreases. This is not the case for the Gaussian approximation nor for the $w = 0$ case. From this we conclude that in order to achieve the saturation of the Δ -entropy, one needs to have a combination of the branching and the broadening.

In the future it will be interesting to investigate the case of the expanding medium as well as to account for coupled evolution of quarks and gluons.

Acknowledgement

This work was partially supported by Polish National Science Centre with grant no. DEC-2017/27/B/ST2/01985. Part of the numerical computations were performed on GPUs at the Helios cluster financed by the Ministry of Education, Youth and Sports of the Czech Republic under the OP RDE grant number CZ.02.2.67/0.0/0.0/16_016/0002357 "Laboratories for Excellent Bachelor and Master Degree Programmes.

A Monte-Carlo algorithm

With the help of the Sudakov form-factors

$$\Delta(p_0^+, t) = \exp \left(-t \left[\int_{|\mathbf{q}| > q_\downarrow} \frac{d^2 \mathbf{q}}{(2\pi)^2} \left(w(\mathbf{q}) + \alpha_s \int_0^{1-\varepsilon} dz 2z \mathcal{K}(\mathbf{q}, z, p_0^+) \right) \right] \right), \quad (17)$$

where the notation $|\mathbf{q}| > q_\downarrow$ should indicate that the integration runs over all \mathbf{q} except those where $|\mathbf{q}| < q_\downarrow$, it can be shown that the following integral equation is equivalent to the integro-differential equation Eq. (1):

$$\begin{aligned} D(x, \mathbf{k}, t) &= D(x, \mathbf{k}, t_0) \frac{\Delta(xp_0^+, t)}{\Delta(xp_0^+, t_0)} \\ &+ \int_{t_0}^t dt' \frac{\Delta(xp_0^+, t)}{\Delta(xp_0^+, t')} \int_{|\mathbf{q}| > q_\downarrow} \frac{d^2 \mathbf{q}}{(2\pi)^2} \int_0^{1-\varepsilon} dz \int \frac{d^2 \mathbf{Q}}{(2\pi)^2} \int_0^1 dy (2\pi)^2 \\ &\left[w(\mathbf{Q}) \delta^{(2)}(\mathbf{k} - (\mathbf{Q} + \mathbf{q})) \delta(x - y) + \alpha_s 2z \mathcal{K}(\mathbf{Q}, z, yp_0^+) \delta^{(2)}(\mathbf{k} - (\mathbf{Q} + z\mathbf{q})) \delta(x - zy) \right] \\ &D(y, \mathbf{q}, t'), \end{aligned} \quad (18)$$

in the simultaneous limits of $\varepsilon \rightarrow 0$ and $q_\downarrow \rightarrow 0$.

The individual terms in Eq. (18) can be associated with probabilities:

- The probability that the fragmentation function at time t gets a contribution from the fragmentation function at time t' without additional splitting or scattering between t' and t (but at t' and t some particle interaction occurs):

$$\frac{\Delta(xp_0^+, t)}{\Delta(xp_0^+, t')}. \quad (19)$$

- The probability density that the fragmentation function at the momentum fraction x and the transverse momentum \mathbf{k} gets a contribution from the fragmentation function at the earlier time t' at the momentum fraction y and the transverse momentum \mathbf{q} via a splitting with momentum fraction z and transverse momentum \mathbf{Q} , where $x = zy$ and $\mathbf{k} = \mathbf{Q} + z\mathbf{q}$:

$$\frac{z \mathcal{K}(\mathbf{Q}, z, yp_0^+)}{\int d^2 \mathbf{Q} \int_0^{1-\varepsilon} dz z \mathcal{K}(\mathbf{Q}, z, yp_0^+)}. \quad (20)$$

Thus, the probability for a splitting with a certain z value (independent of the value of Q) is given as

$$\frac{z \mathcal{K}(z)}{\int_0^{1-\varepsilon} dz' z' \mathcal{K}(z')}, \quad (21)$$

where $\mathcal{K}(z)$ is

$$\mathcal{K}(z) = \int d^2 \mathbf{Q} \mathcal{K}(\mathbf{Q}, z, yp_0^+) \frac{\sqrt{yp_0^+}}{2\pi\sqrt{\hat{q}}} = \frac{f(z)^{5/2}}{(z(1-z))^{3/2}}. \quad (22)$$

- The probability density that the fragmentation function at the transverse momentum \mathbf{k} gets a contribution from the fragmentation function at the earlier time t' at the transverse momentum \mathbf{q} via a scattering with the transverse momentum \mathbf{Q} , where $\mathbf{k} = \mathbf{Q} + \mathbf{q}$:

$$\frac{w(\mathbf{Q})}{\int_{|\mathbf{Q}'|>q_\downarrow} d^2\mathbf{Q}' w(\mathbf{Q}')} . \quad (23)$$

Thus, it is possible to obtain solutions for Eq. (1) via a Monte-Carlo algorithm, where a distribution $D(x, \mathbf{k}, t)$ that obeys Eq. (18) can be obtained by selecting independently of one another a large number N_{ev} of sets (x, \mathbf{k}) , which follow $D(x, \mathbf{k}, t)$.

In each of the N_{ev} cases, the x and \mathbf{k} values are obtained in the following way:

- Some initial values x_0, \mathbf{k}_0 are set together with the time t_0 of the start of the evolution.
- For every set (x_i, \mathbf{k}_i, t_i) , $i \in \mathbb{N}$, a new set $(x_{i+1}, \mathbf{k}_{i+1}, t_{i+1})$ is selected, where $t_{i+1} > t_i$.
- The previous step is repeated until for some time t_j $j \in \mathbb{N}$, it is found that $t_j \geq t$. Then the algorithm gives $x = x_{j-1}$, $\mathbf{k}_j = \mathbf{k}_{j-1}$ and stops.

The selection of a set $(x_{i+1}, \mathbf{k}_{i+1}, t_{i+1})$ from a set (x_i, \mathbf{k}_i, t_i) is done in the following way:

1. Select time t_{i+1} of next splitting/scattering by first choosing a random number $R \in [0, 1]$ from a uniform distribution and then solving the equation

$$R = \frac{\Delta(xp_0^+, t_{i+1})}{\Delta(xp_0^+, t_i)} . \quad (24)$$

The result of this calculation is

$$t_{i+1} = t^* \left(\frac{t_i}{t^*} - \frac{\ln(R)}{\int_0^{1-\varepsilon} dz z \mathcal{K}(z) \frac{1}{\sqrt{x_i}} + t^* \int_{|\mathbf{q}|>q_\downarrow} \frac{d^2\mathbf{q}}{(2\pi)^2} w(\mathbf{q})} \right) . \quad (25)$$

2. Determine whether a splitting or scattering occurs:

This is done, by first selecting a random number $R \in [0, 1]$ from a uniform distribution. If

$$R > \frac{\int_0^{1-\varepsilon} dz z \mathcal{K}(z) \frac{1}{\sqrt{x_i}}}{\int_0^{1-\varepsilon} dz z \mathcal{K}(z) \frac{1}{\sqrt{x_i}} + t^* \int_{|\mathbf{q}|>q_\downarrow} \frac{d^2\mathbf{q}}{(2\pi)^2} w(\mathbf{q})} \quad (26)$$

a scattering occurs, otherwise a splitting.

3. If a splitting occurs, determine x_{i+1} and \mathbf{k}_{i+1} as follows:

- (a) Select z from $\mathcal{K}(z)$ by choosing a random number $R \in [0, 1]$ from a uniform distribution and then solve the equation

$$R = \frac{\int_0^z dz' z' \mathcal{K}(z')}{\int_0^{1-\varepsilon} dz'' z'' \mathcal{K}(z'')} . \quad (27)$$

This equation is solved approximately by first tabulating values of $\int_0^z dz' z' \mathcal{K}(z')$ for a set of z values that is sufficiently dense for the desired accuracy and then searching from this table the z value, which is the closest to the one that solves Eq. (27).

- (b) Select Q from $\mathcal{K}(z, Q)$ by choosing random number $R \in [0, 1]$ from a uniform distribution and solving for $a := \frac{Q^2}{2k_{br}^2}$ the equation

$$R = \frac{\int_0^a da' \sin(a') e^{-a'}}{\int_0^\pi da'' \sin(a'') e^{-a''}} = \frac{1 - (\cos(a) + \sin(a))e^{-a}}{1 + e^{-\pi}}. \quad (28)$$

After selection of a , the value of $Q = \sqrt{2k_{br}^2 a}$ is calculated. While the values of a can assume any positive value, we here constrain the values to the region $a \in [0, \pi]$ in order to avoid the region where $\sin(a)e^{-a}$ becomes negative. Indeed the splitting function in the form of Eq. (2) was deduced in Ref. [26] in the harmonic approximation, which needs corrections at large momentum scales.

- (c) Select the azimuthal angle $\phi \in [0, 2\pi]$ from a uniform distribution.
(d) Obtain x_{i+1} as $x_{i+1} = x_i z$.
(e) Obtain \mathbf{k}_{i+1} as $\mathbf{k}_{i+1} = \mathbf{Q} + z\mathbf{k}_i$ via

$$k_{i+1,x} = Q \cos \phi + z k_{i,x}, \quad (29)$$

$$k_{i+1,y} = Q \sin \phi + z k_{i,y}, \quad (30)$$

where the subscripts x and y denote the respective Cartesian coordinates of the momenta \mathbf{k}_i and \mathbf{k}_{i+1} .

4. If a scattering occurs, determine \mathbf{k}_{i+1} as follows:

- (a) Select Q by choosing from a uniform distribution a random value $R \in [0, 1]$ and then solving for Q the equation

$$R = \frac{\int_{q_\downarrow}^Q d^2 Q' w(\mathbf{Q}')}{\int_{q_\downarrow}^\infty d^2 Q'' w(\mathbf{Q}'')}. \quad (31)$$

For the scattering kernel of the form given in Eq. (6), this equation has the following solution:

$$Q = \frac{q_\downarrow}{\sqrt{1-R}}. \quad (32)$$

- (b) Obtain \mathbf{k}_{i+1} as $\mathbf{k}_{i+1} = \mathbf{Q} + \mathbf{k}_i$.

B Deterministic method

Eq. (10) can be rewritten in the polar coordinates as:

$$\begin{aligned} \frac{\partial}{\partial t} D(x, k, \phi, t) &= \frac{1}{t^*} \int_0^1 dz \mathcal{K}(z) \left[\frac{1}{z^2} \sqrt{\frac{z}{x}} D\left(\frac{x}{z}, \frac{k}{z}, \phi, t\right) \theta(z-x) - \frac{z}{\sqrt{x}} D(x, k, \phi, t) \right] \\ &+ \hat{q} \frac{1}{4} \left[\left(\frac{\partial}{\partial k} \right)^2 + \frac{1}{k} \frac{\partial}{\partial k} + \frac{1}{k^2} \frac{\partial}{\partial \phi} \right] D(x, k, \phi, t). \end{aligned} \quad (33)$$

The initial condition for the $D(x, k, \phi, t)$ is given by

$$D(x, k, \phi, 0) = \begin{cases} \frac{1}{2\pi\sigma^2} \exp\left(-\frac{k^2}{2\sigma^2}\right) & \text{for } x = 1, \\ 0 & \text{for } 0 \leq x < 1, \end{cases} \quad (34)$$

where $\sigma = 1 \text{ GeV}$. The equation is symmetric with respect to the polar angle ϕ , so the corresponding Laplacian simplifies.

In order to get the integrated distribution one needs to calculate the integral:

$$D(t, x) = \int d\phi dk k D(t, x, k, \phi) \quad (35)$$

The equation can be solved directly for the ϕ -integrated distribution, since the ϕ -dependence is trivial.

The terms on RHS of the Eq. (33) are evaluated by central differences (the Laplacian of k with one-sided approximations at the boundaries of the computational domain) and by the box-rule (the integral term):

$$\begin{aligned} \frac{\partial D_{i,j}(t)}{\partial t} &= \frac{\hat{q}}{4} \left(\frac{1}{2k_j \Delta k} (D_{i,j+1}(t) - D_{i,j-1}(t)) + \frac{1}{(\Delta k)^2} (D_{i,j+1}(t) - 2D_{i,j}(t) + D_{i,j-1}(t)) \right) \\ &+ \frac{1}{t^*} \sum_{l=i}^{N_x} \Delta x \mathcal{K}(x_l) \left[\frac{1}{x_l^2} \sqrt{\frac{x_l}{x_i}} D_{(i/l,j/l)}(t) - \frac{x_l}{\sqrt{x_i}} D_{i,j}(t) \right]. \end{aligned} \quad (36)$$

A numerical grid is equidistant and 2-dimensional (we drop the ϕ -dependence due to the symmetry of the problem):

$$x_i = i\Delta x, \quad k_j = j\Delta k, \quad i \in [0, N_x - 1], \quad j \in [0, N_k - 1], \quad \Delta x = \frac{1}{N_x}, \quad \Delta k = \frac{k_{max}}{N_k}. \quad (37)$$

We solve Eq. (36) to obtain the functions $D_{i,j}(t_n) = D(x_i, k_j, t_n)$ at given points x_i, k_j and a time level t_n . The initial condition is given by Eq. (34). The number of grid points for x and k is increased up to $N_x = 10240$ and $N_k = 1000$ with $x \in [0, 1]$ and $k \in [0, 50]$ ($k_{max} = 50$) for the case of $\hat{q} = 1500 \text{ GeV}^2/\text{fm}$, for other \hat{q} we used coarse grid with $N_x = 1024$ and $N_k = 200$.

We use a fourth-order Runge–Kutta method to obtain the numerical solution of the Eq. (36) in time (the Cash–Karp method with the adaptive time stepping [52] is employed). The time

step is being changed according to the following formula:

$$\Delta t = \begin{cases} 0.9\Delta t \left(\frac{\text{TOL}}{E}\right)^{0.2} & \text{for } E < \text{TOL}, \\ 0.9\Delta t \left(\frac{\text{TOL}}{E}\right)^{0.25} & \text{for } E \geq \text{TOL}, \end{cases} \quad (38)$$

where $\text{TOL} = 10^{-6}$ is a tolerance and E is the maximal error in the last step of the embedded Runge–Kutta method. In order to minimise the computational time, the numerical code was parallelized and implemented in NVIDIA CUDA (double precision was used in computations).

References

- [1] B. L. Ioffe, V. S. Fadin and L. N. Lipatov, *Quantum chromodynamics: Perturbative and nonperturbative aspects*, vol. 30. Cambridge Univ. Press, 2010, 10.1017/CBO9780511711817.
- [2] M. Gyulassy and M. Plumer, *Jet Quenching in Dense Matter*, *Phys. Lett.* **B243** (1990) 432–438.
- [3] X.-N. Wang and M. Gyulassy, *Gluon shadowing and jet quenching in A + A collisions at $s^{*(1/2)} = 200\text{-GeV}$* , *Phys. Rev. Lett.* **68** (1992) 1480–1483.
- [4] STAR collaboration, C. Adler et al., *Disappearance of back-to-back high p_T hadron correlations in central Au+Au collisions at $\sqrt{s_{NN}} = 200\text{-GeV}$* , *Phys. Rev. Lett.* **90** (2003) 082302, [nucl-ex/0210033].
- [5] ATLAS collaboration, G. Aad et al., *Observation of a Centrality-Dependent Dijet Asymmetry in Lead-Lead Collisions at $\sqrt{s_{NN}} = 2.77\text{ TeV}$ with the ATLAS Detector at the LHC*, *Phys. Rev. Lett.* **105** (2010) 252303, [1011.6182].
- [6] P. Caucal, E. Iancu, A. H. Mueller and G. Soyez, *Vacuum-like jet fragmentation in a dense QCD medium*, *Phys. Rev. Lett.* **120** (2018) 232001, [1801.09703].
- [7] P. Caucal, E. Iancu and G. Soyez, *Deciphering the z_g distribution in ultrarelativistic heavy ion collisions*, 1907.04866.
- [8] S. Schlichting and D. Teaney, *The First fm/c of Heavy-Ion Collisions*, *Ann. Rev. Nucl. Part. Sci.* **69** (2019) 447–476, [1908.02113].
- [9] R. Baier, D. Schiff and B. G. Zakharov, *Energy loss in perturbative QCD*, *Ann. Rev. Nucl. Part. Sci.* **50** (2000) 37–69, [hep-ph/0002198].
- [10] R. Baier, A. H. Mueller, D. Schiff and D. T. Son, *'Bottom up' thermalization in heavy ion collisions*, *Phys. Lett.* **B502** (2001) 51–58, [hep-ph/0009237].
- [11] S. Jeon and G. D. Moore, *Energy loss of leading partons in a thermal QCD medium*, *Phys. Rev.* **C71** (2005) 034901, [hep-ph/0309332].
- [12] B. G. Zakharov, *Fully quantum treatment of the Landau-Pomeranchuk-Migdal effect in QED and QCD*, *JETP Lett.* **63** (1996) 952–957, [hep-ph/9607440].
- [13] B. G. Zakharov, *Radiative energy loss of high-energy quarks in finite size nuclear matter and quark - gluon plasma*, *JETP Lett.* **65** (1997) 615–620, [hep-ph/9704255].
- [14] B. G. Zakharov, *Transverse spectra of radiation processes in-medium*, *JETP Lett.* **70** (1999) 176–182, [hep-ph/9906536].

- [15] R. Baier, Y. L. Dokshitzer, S. Peigne and D. Schiff, *Induced gluon radiation in a QCD medium*, *Phys. Lett.* **B345** (1995) 277–286, [hep-ph/9411409].
- [16] R. Baier, Y. L. Dokshitzer, A. H. Mueller, S. Peigne and D. Schiff, *The Landau-Pomeranchuk-Migdal effect in QED*, *Nucl. Phys.* **B478** (1996) 577–597, [hep-ph/9604327].
- [17] P. B. Arnold, G. D. Moore and L. G. Yaffe, *Photon and gluon emission in relativistic plasmas*, *JHEP* **06** (2002) 030, [hep-ph/0204343].
- [18] J. Ghiglieri, G. D. Moore and D. Teaney, *Jet-Medium Interactions at NLO in a Weakly-Coupled Quark-Gluon Plasma*, *JHEP* **03** (2016) 095, [1509.07773].
- [19] C. A. Salgado and U. A. Wiedemann, *Calculating quenching weights*, *Phys. Rev.* **D68** (2003) 014008, [hep-ph/0302184].
- [20] K. Zapp, G. Ingelman, J. Rathsman, J. Stachel and U. A. Wiedemann, *A Monte Carlo Model for 'Jet Quenching'*, *Eur. Phys. J.* **C60** (2009) 617–632, [0804.3568].
- [21] N. Armesto, L. Cunqueiro and C. A. Salgado, *Q-PYTHIA: A Medium-modified implementation of final state radiation*, *Eur. Phys. J.* **C63** (2009) 679–690, [0907.1014].
- [22] B. Schenke, C. Gale and S. Jeon, *MARTINI: An Event generator for relativistic heavy-ion collisions*, *Phys. Rev.* **C80** (2009) 054913, [0909.2037].
- [23] I. P. Lokhtin, A. V. Belyaev and A. M. Snigirev, *Jet quenching pattern at LHC in PYQUEN model*, *Eur. Phys. J.* **C71** (2011) 1650, [1103.1853].
- [24] J. Casalderrey-Solana, D. C. Gulhan, J. G. Milhano, D. Pablos and K. Rajagopal, *A Hybrid Strong/Weak Coupling Approach to Jet Quenching*, *JHEP* **10** (2014) 019, [1405.3864].
- [25] H. Liu, K. Rajagopal and U. A. Wiedemann, *Calculating the jet quenching parameter from AdS/CFT*, *Phys. Rev. Lett.* **97** (2006) 182301, [hep-ph/0605178].
- [26] J.-P. Blaizot, F. Dominguez, E. Iancu and Y. Mehtar-Tani, *Probabilistic picture for medium-induced jet evolution*, *JHEP* **06** (2014) 075, [1311.5823].
- [27] J.-P. Blaizot, L. Fister and Y. Mehtar-Tani, *Angular distribution of medium-induced QCD cascades*, *Nucl. Phys.* **A940** (2015) 67–88, [1409.6202].
- [28] K. Kutak, W. Paczek and R. Straka, *Solutions of evolution equations for medium-induced QCD cascades*, *Eur. Phys. J.* **C79** (2019) 317, [1811.06390].
- [29] C. Andres, L. Apolinario and F. Dominguez, *Medium-induced gluon radiation with full resummation of multiple scatterings for realistic parton-medium interactions*, *JHEP* **07** (2020) 114, [2002.01517].

- [30] A. H. Mueller, B. Wu, B.-W. Xiao and F. Yuan, *Probing Transverse Momentum Broadening in Heavy Ion Collisions*, *Phys. Lett.* **B763** (2016) 208–212, [1604.04250].
- [31] A. Mueller, B. Wu, B.-W. Xiao and F. Yuan, *Medium Induced Transverse Momentum Broadening in Hard Processes*, *Phys. Rev. D* **95** (2017) 034007, [1608.07339].
- [32] B. Zakharov, *Radiative parton energy loss and baryon stopping in AA collisions*, *JETP Lett.* **110** (2019) 375–381, [1908.03723].
- [33] B. Zakharov, *Radiative p_{\perp} -broadening of fast partons in an expanding quark-gluon plasma*, 2003.10182.
- [34] B. Zakharov, *Updated analysis of jet quenching at RHIC and LHC within the light cone path integral approach*, 2007.09772.
- [35] E. Iancu, P. Taelis and B. Wu, *Jet quenching parameter in an expanding QCD plasma*, *Phys. Lett. B* **786** (2018) 288–295, [1806.07177].
- [36] S. P. Adhya, C. A. Salgado, M. Spousta and K. Tywoniuk, *Medium-induced cascade in expanding media*, *JHEP* **07** (2020) 150, [1911.12193].
- [37] P. Aurenche, F. Gelis and H. Zaraket, *A Simple sum rule for the thermal gluon spectral function and applications*, *JHEP* **05** (2002) 043, [hep-ph/0204146].
- [38] J.-P. Blaizot, Y. Mehtar-Tani and M. A. C. Torres, *Angular structure of the in-medium QCD cascade*, *Phys. Rev. Lett.* **114** (2015) 222002, [1407.0326].
- [39] B. Muller and A. Schafer, *Entropy Creation in Relativistic Heavy Ion Collisions*, *Int. J. Mod. Phys. E* **20** (2011) 2235–2267, [1110.2378].
- [40] K. Kutak, *Gluon saturation and entropy production in proton–proton collisions*, *Phys. Lett. B* **705** (2011) 217–221, [1103.3654].
- [41] R. Peschanski, *Dynamical entropy of dense QCD states*, *Phys. Rev. D* **87** (2013) 034042, [1211.6911].
- [42] A. Kovner and M. Lublinsky, *Entanglement entropy and entropy production in the Color Glass Condensate framework*, *Phys. Rev. D* **92** (2015) 034016, [1506.05394].
- [43] D. Neill and W. J. Waalewijn, *Entropy of a Jet*, *Phys. Rev. Lett.* **123** (2019) 142001, [1811.01021].
- [44] A. Kovner, M. Lublinsky and M. Serino, *Entanglement entropy, entropy production and time evolution in high energy QCD*, *Phys. Lett. B* **792** (2019) 4–15, [1806.01089].
- [45] N. Armesto, F. Dominguez, A. Kovner, M. Lublinsky and V. Skokov, *The Color Glass Condensate density matrix: Lindblad evolution, entanglement entropy and Wigner functional*, *JHEP* **05** (2019) 025, [1901.08080].

- [46] P. Hanus, A. Mazeliauskas and K. Reygers, *Entropy production in pp and Pb-Pb collisions at energies available at the CERN Large Hadron Collider*, *Phys. Rev. C* **100** (2019) 064903, [1908.02792].
- [47] E. Gotsman and E. Levin, *High energy QCD: multiplicity distribution and entanglement entropy*, 2006.11793.
- [48] Y. Hagiwara, Y. Hatta, B.-W. Xiao and F. Yuan, *Classical and quantum entropy of parton distributions*, *Phys. Rev. D* **97** (2018) 094029, [1801.00087].
- [49] G. Ramos and M. Machado, *Determination of entanglement entropy in elastic scattering using the model-independent method for hadron femtoscopy*, *Phys. Rev. D* **102** (2020) 034019, [2007.09744].
- [50] H. Duan, C. Akkaya, A. Kovner and V. V. Skokov, *Entanglement, partial set of measurements, and diagonality of the density matrix in the parton model*, *Phys. Rev. D* **101** (2020) 036017, [2001.01726].
- [51] B. Chen, Y. Zhu, J. Hu and J. C. Principe, *System Parameter Identification. Information Criteria and Algorithms*. Elsevier, 2013, <https://doi.org/10.1016/C2012-0-01233-1>.
- [52] J. R. Cash and A. H. Karp, *A variable order runge-kutta method for initial value problems with rapidly varying right-hand sides*, *ACM Trans. Math. Softw.* **16** (Sept., 1990) 201222.